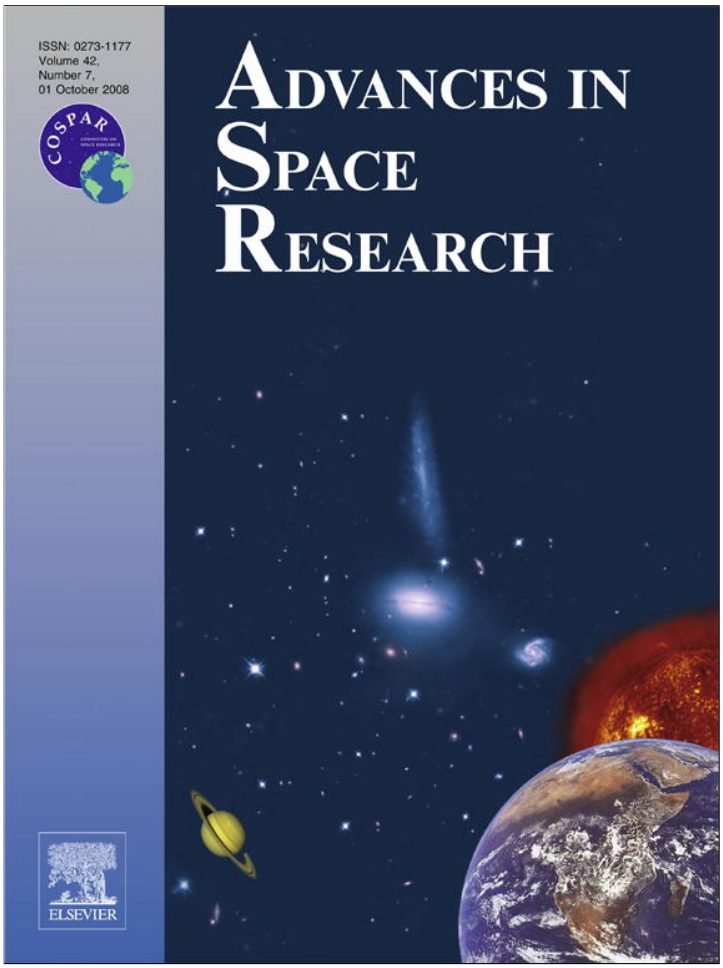

Available online at www.sciencedirect.com
ScienceDirect
Advances in Space Research 42 (2008) 1246–1252
ADVANCES IN SPACE RESEARCH (a COSPAR publication)
www.elsevier.com/locate/asr

Mesospheric doppler wind measurements from Aura Microwave Limb Sounder (MLS)

Dong L. Wu [a,*], Michael J. Schwartz [a], Joe W. Waters [a], Varavut Limpasuvan [b], Qian Wu [c], Timothy L. Killeen [c]

[a] Jet Propulsion Laboratory, California Institute of Technology, Pasadena, CA 91109, USA
[b] Department of Chemistry and Physics, Coastal Carolina University, Conway, SC 29528, USA
[c] High Altitude Observatory, National Center for Atmospheric Research, Boulder, CO 80303, USA

Received 23 October 2006; received in revised form 25 April 2007; accepted 7 June 2007

Abstract

This paper describes a microwave limb technique for measuring Doppler wind in the Earth's mesosphere. The research algorithm has been applied to Aura Microwave Limb Sounder (MLS) 118.75 GHz measurements where the O_2 Zeeman lines are resolved by a digital autocorrelation spectrometer. A precision of ~17 m/s for the line-of-sight (LOS) wind is achieved at 80–92 km, which corresponds to radiometric noise during 1/6 s integration time. The LOS winds from Aura MLS are mostly in the meridional direction at low- and mid-latitudes with vertical resolution of ~8 km. This microwave Doppler technique has potential to obtain useful winds down to ~40 km of the Earth's atmosphere if measurements from other MLS frequencies (near H_2O, O_3, and CO lines) are used. Initial analyses show that the MLS winds from the 118.75 GHz measurements agree well with the TIDI (Thermosphere Ionosphere Mesosphere Energetics and Dynamics Doppler Interferometer) winds for the perturbations induced by a strong quasi 2-day wave (QTDW) in January 2005. Time series of MLS winds reveal many interesting climatological and planetary wave features, including the diurnal, semidiurnal tides, and the QTDW. Interactions between the tides and the QTDW are clearly evident, indicating possible large tidal structural changes after the QTDW events dissipate.

Keywords: Doppler wind; Microwave radiometry; Mesosphere; Tides; Planetary waves

1. Introduction

Dynamics in the Earth's mesosphere and lower thermosphere (MLT) are complex and lack understanding because of large variability. This altitude region plays a critical role in coupling the neutral and ionized parts of the Earth's atmosphere, which is vulnerable to forcings from the lower atmosphere, local instability, and solar activity. Over the past ~15 years, observations of global MLT winds have been relying mostly on visible airglow techniques, such as UARS HRDI (Upper Atmosphere Research Satellite High Resolution Doppler Imager) (Hays et al., 1993), and TIDI (Thermosphere Ionosphere Mesosphere Energetics and Dynamics Doppler Interferometer) (Killeen et al., 1999). These airglow techniques are limited largely to daylight hours as nightglow retreat to a narrow layer, making incomplete coverage in local time, where the diurnal variation is large.

This paper describes a microwave technique for measuring winds in the Earth's mesosphere, which can provide wind profiles during both day and night. Doppler wind measurements at microwave frequencies have been made with ground-based passive techniques for planetary (e.g., Lellouch et al., 1991) and Earth's (Clancy and Muhleman, 1993) atmospheres, and with ground-based and airborne Doppler radar techniques from cloud scattering. Here, we apply the passive technique to remote

* Corresponding author. Tel.: +1 818 393 1954; fax: +1 818 393 5065.
E-mail address: Dong.L.Wu@jpl.nasa.gov (D.L. Wu).

0273-1177/$34.00
doi:10.1016/j.asr.2007.06.014

sensing of mesospheric winds using the 118.75 GHz O_2 emission lines measured by the Microwave Limb Sounder (MLS) instrument on NASA Aura satellite (Waters et al., 2006). Although Aura MLS is not a wind instrument, it can determine a small Doppler shift with high precision and accuracy. In addition, emission lines from limb viewing yield a much greater signal-to-noise ratio in wind sensitivity than absorption lines from nadir viewing. Launched in July 2004, the MLS 118 GHz radiometer has been very stable and the precision of the line-of-light (LOS) wind speed is estimated to be ~17 m/s for each 1/6 s integration. Aura is a polar satellite at a 700-km circular, sun-synchronous orbit with 98.2° inclination. The MLS antenna points forward in the satellite moving direction slightly (0.04°) off from the orbital plane. Hence, the LOS direction is primarily meridional, varying from 8.2° with respect to the North at the equator to 16.5° at 60° latitudes. The retrieved LOS winds are in the northeast direction for ascending orbits but change to the southeast direction for descending orbits.

2. MLS wind sensitivity at 118.75 GHz

The 118.75 GHz oxygen lines measured by MLS contain three Zeeman components, (σ^-, π, σ^+), where the σ^- and σ^+ components are often dominant, as seen in Fig. 1, and separated by ~0.5 MHz from the central π component for a geomagnetic field of ~35 T (Schwartz et al., 2006). Thus, the line width in the upper mesosphere, dominated by the thermal Doppler width (~0.21 MHz at 200 K), is comparable to the frequency separation between the σ^- and σ^+ components. To resolve these Zeeman components, the Aura MLS employs a digital autocorrelation spectrometer (DACS) of 0.1 MHz resolution with ~10 MHz bandwidth centered at 118.75 GHz. The DACS single channel noise is ~12 K for a minor frame (MIF), which has a fixed 1/6 s data integration time. The MLS latitude coverage ranges from 82°S to 82°N and adjacent limb scans are separated by ~165 km along track. The nominal limb scan starts from the surface to ~92 km with emphasis on the lower atmosphere, producing dense sampling (~0.37 km/MIF) below at tangent heights <25 km, moderate sampling (~1 km/MIF) at 25–65 km, and coarse sampling (~2.5 km/MIF) at 65–92 km (Waters et al., 2006). At the top of each scan, there are ~12 MIFs that can be used for determining mesospheric winds with the DACS. The observed O_2 Zeeman lines remain quite strong (~20 K) at 110 km but unfortunately the nominal MLS operation only goes up ~92 km.

Fig. 1a shows the modeled 85 km O_2 spectrum for MLS DACS channels, where the σ^- and σ^+ components are stronger than the π component. Except in the tropical region, most of the 118.75 GHz DACS measurements look like this spectrum, and the frequency separation between the σ^- and σ^+ components is proportional to geomagnetic field strength. Benefited from the Zeeman splitting, the two σ^- and σ^+ lines give MLS better sensitivity to Doppler shifts than otherwise with a single line. As shown in Fig. 1b, Doppler shifts from a 100 m/s wind can induce radiance differences of ~50 K peak-to-peak in this case, which is readily detectable by the MLS DACS.

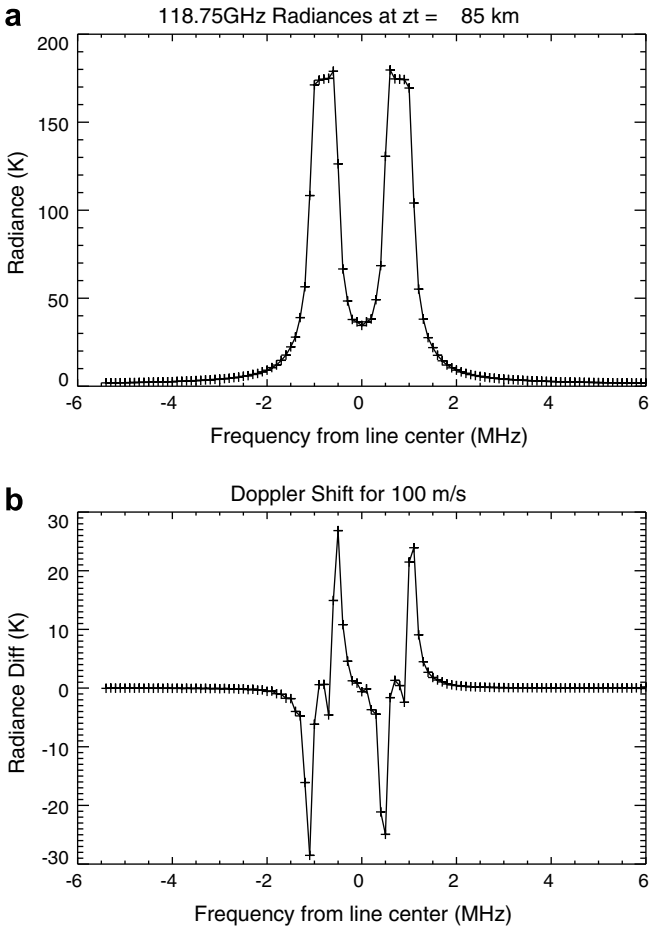

Fig. 1. (a) Modeled Zeeman O_2 radiance spectrum with respect to the line center at 118.75 GHz. (b) Radiance perturbations due to a frequency shift equivalent to 100 m/s LOS wind speed.

Vertical resolution of MLS LOS winds is determined mostly by the vertical weighting function of limb geometry and the width of instrument field of view (FOV). For an infinitely narrow limb array, the weighting function is sharply peaked at the tangent point (as shown with the dashed lines in Fig. 2), known as the Abel kernel, and the exponential decrease of O_2 density helps further sharpen the Abel kernel. The instrument FOV is relatively broad for the 118 GHz radiometer, which becomes the ultimate limiting factor of MLS vertical resolution. The convolution of the two (as shown with the solid lines in Fig. 2) give a layer thickness of ~8 km. In this research algorithm, we did not make any inversion on the LOS winds for a finer vertical resolution. Instead, we report the LOS winds directly as a function of associated tangent height, and therefore these winds are independent of each other but should be interpreted as an average over the 8-km layer centered at 2 km above their tangent height.

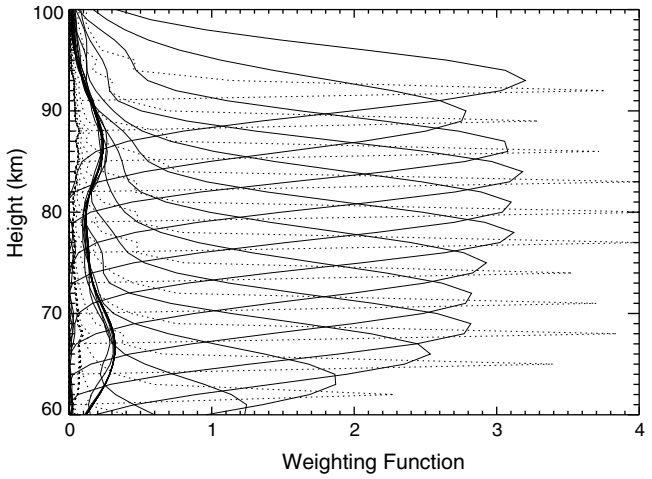

Fig. 2. Weighting functions of the LOS wind for different tangent heights between 60 and 90 km during MLS nominal scan. The dotted curves represent the functions as if it has an infinitely narrow FOV whereas the solid curves represent realistic MLS WFs for a 5.8 km FOV. Note that the WF peak is slightly (~2 km) higher than the pointing tangent height and the vertical resolution is defined by the half-peak width (~8 km).

3. Retrieval method

3.1. Empirical forward models

Determining Doppler shifts of the O_2 Zeeman lines requires an accurate radiance forward model for MLS DACS measurements, which is found to be sophisticated and computation-costly. To make practical determination of Doppler shifts from the DACS, we developed a set of empirical models based on the DACS radiance measurements. They are the averaged radiance profiles for each $5° \times 10°$ Lat–Lon bin (separated for ascending and descending orbits) and for every 2 km in tangent heights between 60 and 100 km. Since MLS limb scans are stable and repeatable from orbit to orbit, we neglect small pointing error that may occur between orbits. In addition, the radiance sensitivities to pointing/temperature and Doppler shift are orthogonal to each other, and the slight pointing/temperature error would not significantly contaminate the sensitivity to Doppler shifts. Finally, we remove systematic Doppler shifts due to satellite motion and the Earth's rotation, which can be determined accurately from spacecraft attitude data on a scan-by-scan basis. The sum of satellite and Earth's rotation is found to be nearly constant at 6868 ± 0.5 m/s when projected onto the MLS viewing direction.

The last step is to determine the zero wind for each empirical model. Since MLS has no frequency drift problem, which was common for HRDI and WINDII (Wind Imaging Interferometer) instruments, zero winds are relatively straightforward to obtain. For each empirical model, we average the first year of wind retrievals and set the averages to zero to correct potential biases from the model. It is assumed that atmospheric variability would average down substantially to near zero over a long period of time. These corrections for zero wind are typically around 20 m/s and would require further validation against correlative measurements. Similar approaches have been applied for finding zero winds in UARS HRDI and WINDII data (Burrage et al., 1996; Gault et al., 1996), and the zero wind determined with this approach was found to be accurate to <5 m/s.

3.2. Estimated precision

Fig. 3 gives the precision estimated from the MLS wind retrieval for 1/6-s integration. The precision varies slightly from profile to profile but is typically leveled at 17–20 m/s at 83–92 km and degrades to ~60 m/s at 70 km. The error increase at lower altitudes is partly due to the finite bandwidth (~10 MHz) of the DACS, but fundamentally the wind error is dictated by radiometric noise and integration time. Wind retrievals at altitudes below 70 km can be made from measurements with other MLS filterbanks for the 118.75 GHz O_2, 183.31 GHz H_2O, 235.71 GHz O_3, and 230.54 GHz CO lines, of which the technique will be described in a separate paper.

To verify MLS wind sensitivity, we compared MLS LOS winds to TIDI measurements in January 2005 when a quasi-2-day wave (QTDW) strongly perturbed the meridional wind. Limpasuvan et al. (2005) studied a QTDW event in January–February 2005 using MLS temperature, H_2O, CO, and LOS wind data, and found that the temperature and wind amplitudes reached as large as 9 K and 50 m/s near 90 km. Since TIDI and MLS samplings are rarely collocated, to compare their winds we first reconstruct the QTDW perturbations using TIDI (nighttime cold-side) vector winds and then projected them onto the MLS LOS direction, which we call the TIDI LOS wind. As shown in Fig. 4, the TIDI LOS winds agree well with the MLS LOS winds, showing good one-to-one correlation

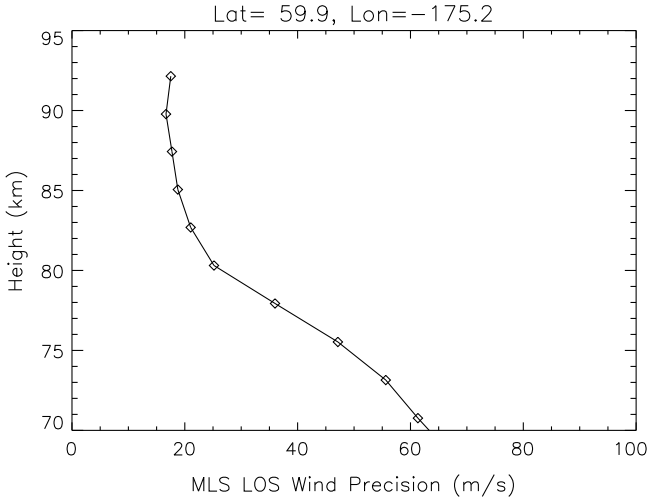

Fig. 3. Estimated precision of MLS LOS wind from the retrieval at (59.9°N, 175.2°W) with the 118 GHz DACS radiances.

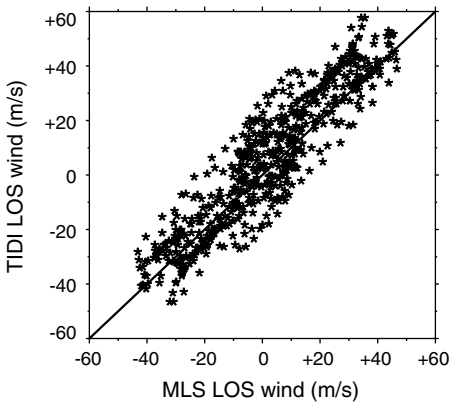

Fig. 4. TIDI wind perturbations interpolated onto the MLS LOS direction (namely, TIDI LOS wind) in comparison with MLS LOS wind perturbations during 24–27 January 2005. A strong global 2-day wave event occur during this period of time with wave amplitudes exceeding 40 m/s.

over the range of oscillations induced by the global QTDW.

4. Climatological and planetary wave features

Dynamics in the mesosphere are subject to frequent planetary wave perturbations, such as the diurnal, semidiurnal migrating tides and the QTDW. The observed LOS winds can be expressed as a sum of the mean wind plus planetary waves, namely,

$$V = \bar{V} + \sum_i V_i' \sin 2\pi(\sigma_i t/24 - s_i\lambda/360 + \varphi_i)$$

for frequency and wavenumber (σ, s), where time t and longitude λ are in hours and degrees, and ϕ is phase of the waves. Beside the waves excited by forcings in the troposphere and stratosphere, many planetary waves can result from wave–wave interactions as a second or third harmonic (Palo et al., 1999). Some of these planetary waves, if associated with large perturbations in the meridional wind, can be readily observed in the MLS LOS wind data, and wave amplitudes can be extracted with the running least-squared fitting method (Wu et al., 1995).

4.1. The diurnal migrating tide

The westward propagating diurnal tide, $(1, -1)$, is a well-known wave feature in the MLT region, producing large disturbances in the meridional wind in the tropics and subtropics. The meridional component of this tidal wave has a primary mode that is asymmetric about the equator with peak amplitudes at ~20° latitudes. It is excited from the solar heating in the troposphere and stratosphere, and propagates upward with a vertical wavelength between 20 and 30 km. Because the diurnal tide

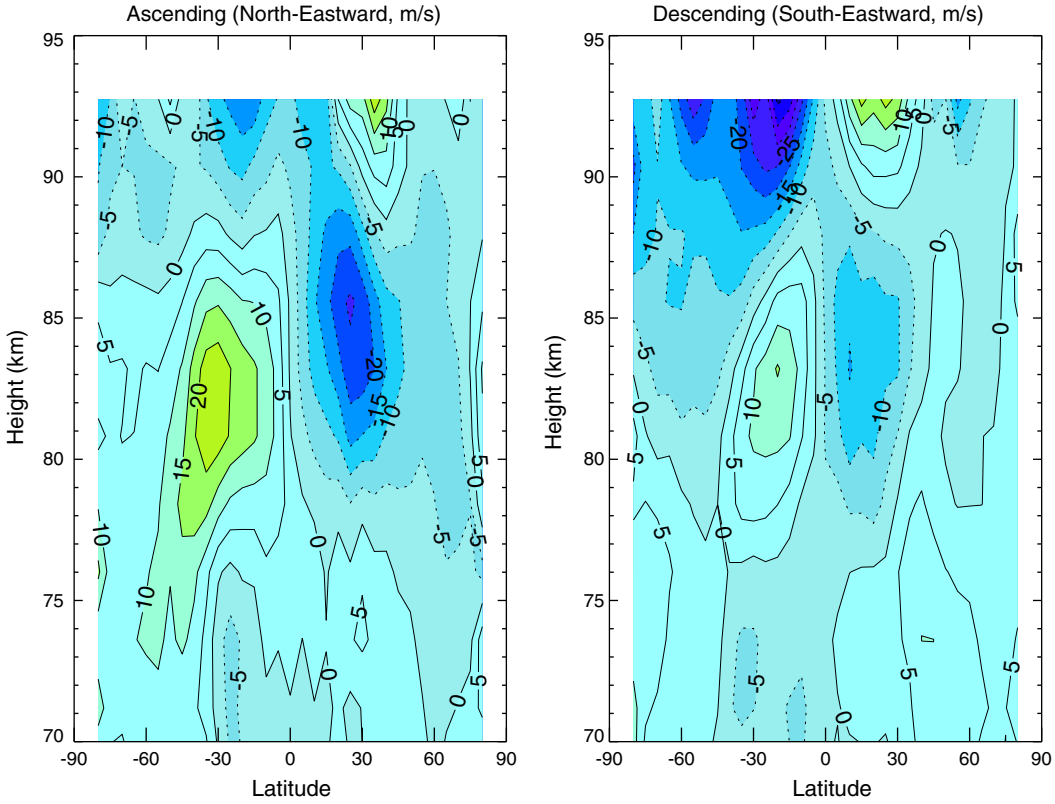

Fig. 5. Ascending and descending zonal means of the MLS LOS wind (mostly in the meridional direction at low- and mid-latitudes). The diurnal tide induces large (±20 m/s) perturbations in the meridional wind, showing diverging and converging motions near the equator. Since MLS LOS wind reverses its meridional direction from ascending to descending orbits, the diurnal meridional wind perturbations exhibit the same sign in both ascending and descending means.

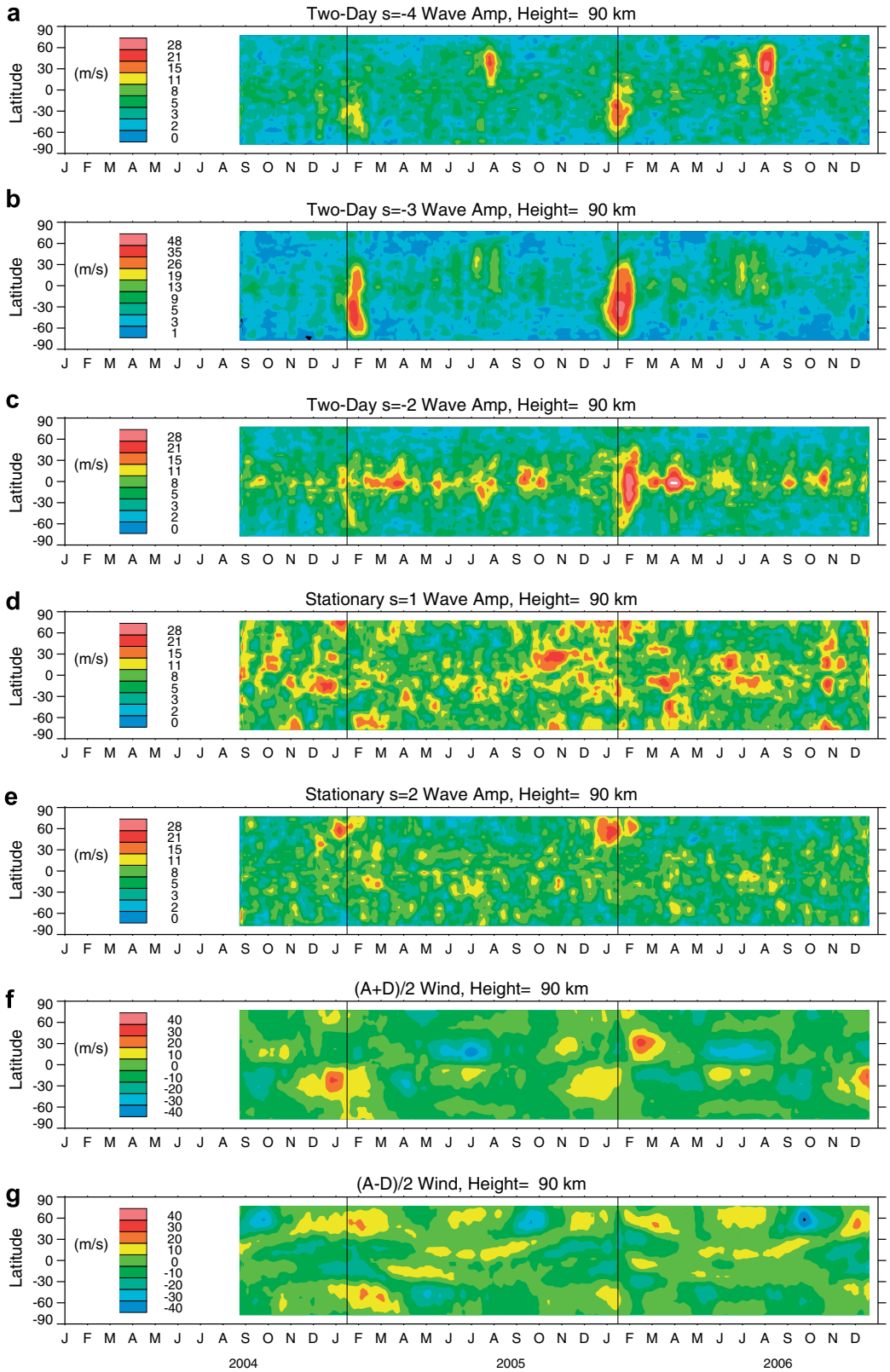

Fig. 6. Time series of six wave components: (a–c) 48 h $s = -4, -3, -2$ wave amplitudes, (d, e) stationary $s = 1$ and $s = 2$ amplitudes, (f, g) $(A + D)/2$ and $(A - D)/2$ average winds at 90 km. The wave amplitudes are derived from descending orbits using the least-square fit method on running 5-day windows. In addition, a 10-day smoothing is applied to the derived wave amplitudes in these plots. The $(A + D)/2$ and $(A - D)/2$ winds can be interpreted mostly as the diurnal and semidiurnal winds, respectively (see text for the details). January 15 is marked by the vertical lines as a reference to compare the timing of variations associated with the QTDW events.

travels westward at the same phase speed as the sun migrates, from the view of a sun-synchronous sensor, it appears as a fixed pattern in the latitude–height plot except that the pattern flips sign between ascending (A) and descending (D) measurements. MLS LOS wind always flips sign of the meridional wind when it changes from A to D orbit, and therefore one would expect that the diurnal tidal structure appear similarly in the A and D latitude–height plots. Indeed, on 28 March 2006, the daily LOS winds averaged for A and D orbits exhibit similar cellular structures at lower latitudes, showing converging and diverging flows at the equator. The flow direction change with height reflects the tidal vertical wavelength (20–30 km). Since the mean meridional winds are small compared to the tidal amplitude at these altitudes, the observed meridional wind variability is dominated by the tidal oscillation. As shown in Fig. 5, the wind oscillations peak at ~30° latitudes is consistent with the primary mode of the diurnal tide. The inferred wavelength and tidal structure are also consistent with the HRDI observations and model simulations at these altitudes (Hays and Wu, 1994; Hagan et al., 1999).

4.2. Planetary waves

Beside the diurnal tide, the semidiurnal tide can also be important in the MLT region. Simultaneous presence of the diurnal and semidiurnal tides could make the interpretation of the A or D measurements complicated because of aliasing problems. Since the local time difference between A and D nodes is ~12 h for the sun-synchronous Aura orbit, the diurnal/semidiurnal components would be more pronounced in the $A - D$ and $A + D$ winds than in A and D themselves. As shown in Fig. 5, the diurnal tide would appear as a similar structure for both A and D measurements, and thus the $(A + D)/2$ wind can be interpreted mainly as the meridional diurnal amplitude. The $(A + D)/2$ wind will remove the semidiurnal meridional wind. If the mean winds and the semidiurnal zonal wind are negligible, this would be a reasonable assumption. At low-latitudes, the mean meridional wind is generally small. The mean and semidiurnal zonal wind can sometimes be significant but reduced substantially after projected onto the MLS LOS direction. Contributions of the zonal component may become important at high-latitudes as the MLS LOS direction tilts more toward the zonal direction. Thus, variations of the low-latitude $(A + D)/2$ wind in Fig. 6 are mostly due to the meridional component of the diurnal tide. The converging and diverging flows of the $(A + D)/2$ wind near the equator is consistent with the tidal wind structure. Phase changes occur often in the $(A + D)/2$ wind, reflecting major structural changes in the diurnal tide, which appear to be dramatic after the QTDW events dissipate.

On the other hand, the $(A - D)/2$ wind removes the diurnal and zonal components but keeps the semidiurnal components at low- and mid-latitudes. Since the mean meridional wind is weak in general, the $(A - D)/2$ wind is dominated by the meridional wind oscillations induced by the semidiurnal tide. Even at 60° latitudes where the local time difference is ~10 h, the $(A - D)/2$ wind remains as a good proxy for the semidiurnal component except with a reduced amplitude. The seasonal variation of the $(A - D)/2$ wind amplitude observed by MLS is consistent with the semidiurnal tide observed by HRDI (Burrage et al., 1995) and ground-based radars (Mason et al., 2002), showing large oscillations in September and January–February at the Northern Hemisphere (NH) mid-latitudes and in February–March at Southern Hemisphere (SH) mid-latitudes. In the tropics the $(A - D)/2$ wind shows double latitude bands and appears to have oscillations with ~15 m/s in amplitude all the time. Because both amplitude and phase of the semidiurnal tide may vary with time, it is difficult for MLS to extract these variations unambiguously. Further investigations with correlative observations (e.g., MLS and SABER temperature, TIDI winds) and models can help to confirm and better understand the tidal variability.

Interactions between the QTDW and the diurnal tide has profound impacts on MLT dynamics since both waves are salient global oscillations in the region. The QTDW is a strong $s = -3$ (westward propagating) perturbation in the upper atmosphere that often occurs near the solstice and can persist for 15–30 days (e.g., Wu et al., 1995), while the diurnal tide is constantly forced by solar heating but exhibits large variability in the MLT region by interacting with the mean wind, gravity waves and other planetary waves (Hagan et al., 1999). In a model simulation study, Palo et al. (1999) found that non-linear interactions between the QTDW and the migrating tides could cause a significant decrease in tidal amplitudes along with a number of additional planetary waves that would not be present without the QTDW. From radar and satellite observations, Nozawa et al. (2003) and Riggin et al. (2004) found that a significant part of the QTDW power is spread out to $s = -2$ and $s = -4$, revealing complex nature of the QTDW and interactions with instabilities and the environment.

As shown in Fig. 6, the QTDW always exhibits a larger $s = -3$ amplitude in January than in June–August with the peak amplitude centered around a southern mid-latitude. The event in January 2006 is stronger than the January 2005 case (Limpasuvan et al., 2005), reaching the peak amplitude of ~65 m/s at 40°S. Significant QTDW power is also found in the $s = -2$ and $s = -4$ components. The $s = -2$ wave resides mostly in the equatorial region while the $s = -4$ wave shows slightly larger amplitudes in June–August than in January with preferential occurrence at summertime mid-latitudes. Prior to the QTDW events, there is a significant stationary $s = 2$ wave at high northern latitudes, which appears to be also stronger in 2006. It is not clear whether the stationary $s = 2$ wave is related to excitation or amplification of the QTDW. The stationary $s = 1$ wave amplitude is patchy and transient in general. It appears to be clustered in two subtropical latitude bands with small amplitudes near the equator, which could

manifest itself as non-migrating tides from interactions of the diurnal tide and planetary waves (Talaat and Lieberman, 1999). Further studies are needed to identify the non-migrating tidal components and their dominant modes. Finally, the $(A + D)/2$ and $(A - D)/2$ winds, mostly the diurnal and semidiurnal components, experience large structural changes after the QTDW events dissipate, showing a reversal in the 90 km $(A + D)/2$ wind from converging to diverging flow at the equator. The QTDW interactions with the tides remain as a very interesting research topic in years to come. With MLS wind measurements, we can better quantify and understand the coupling processes that would not be resolved with temperature observations only.

5. Summary and future work

We have described a technique for measuring mesospheric wind from the 118.75 GHz O_2 emission lines. The research algorithm has been applied to Aura MLS limb radiances and a ~17 m/s precision is achieved for the LOS wind measurements with 1/6 s integration time. The LOS wind is mostly in the meridional direction at low- and mid-latitudes with vertical resolution of ~8 km. The MLS LOS wind agrees well with the TIDI wind during the period when a strong QTDW event occurred.

Initial analyses of MLS LOS winds reveal many interesting climatological and planetary wave features, including the diurnal and semidiurnal tides and the QTDW. The observed global morphology of the tides and planetary waves is generally consistent with the past observations from HRDI and WINDII. Interactions between the tides and the QTDW are clearly evident in the MLS wind time series, indicating possible large tidal structural changes after the QTDW events dissipate. Further investigations are needed to quantify these interactions and changes in wave structures as these variabilities are very important to MLT dynamics.

For the future work, we would like to extend MLS wind measurements down to ~40 km using other spectral channels. In addition to the 118.75 GHz O_2 lines, MLS can also resolve the 183.31 GHz H_2O, 230.54 GHz CO, and 235.71 GHz O_3 lines with the high-resolution DACS and low-resolution filterbanks. Each of these spectral lines has a different wind sensitivity in terms of the best height range. By combining these wind sensitivities, we will be able to obtain useful wind data for the entire altitude range between 40 and 92 km. The Doppler winds in the upper stratosphere and lower mesosphere have not measured previously by HRDI due to limitation in airglow techniques.

The Doppler wind techniques with microwave radiometry continue to benefit remote sensing of planetary atmospheres, and they work particularly well for the planets or moons with a thin atmosphere such as Mars and Titan. The CO gas is abundant in these atmospheres and extends to a very high altitude, which makes the microwave technique more attractive to measure their atmospheric winds from an orbiting satellite.

Acknowledgments

This research was conducted at the Jet Propulsion Laboratory, California Institute of Technology, under a contract with the National Aeronautics and Space Administration. We thank the MLS team for operating the instrument and making the data set available for this study. We thank Drs. Dennis Riggin and Scott Pale for valuable discussions on the 2-day wave analysis.

References

Burrage, M.D., Wu, D.L., Skinner, W.R., et al. Latitude and seasonal dependence of the semidiurnal tide observed by the high-resolution Doppler imager. J. Geophys. Res. 100, 11313–11321, 1995.

Burrage, M.D., Skinner, W.R., Gell, D.A., et al. Validation of mesosphere and lower thermosphere winds from the high resolution Doppler imager on UARS. J. Geophys. Res. 101, 10365–10392, 1996.

Clancy, R.T., Muhleman, D.O. in: Janssen, M.A. (Ed.), Atmospheric Remote Sensing Microwave Radiometry. Wiley, New York, pp. 383–496, 1993 (Chapter 7).

Gault, W.A., Thuillier, G., Shepherd, G.G., et al. Validation of O(1S) wind measurements by WINDII: the wind imaging interferometer on UARS. J. Geophys. Res. 101, 10405–10443, 1996.

Hagan, M.E., Burrage, M.D., Forbes, J.M., et al. GSWM-98: results for migrating solar tides. J. Geophys. Res. 104, 6813–6828, 1999.

Hays, P.B., Abreu, V.J., Dobbs, M.E., et al. The high-resolution Doppler imager on the upper-atmosphere research satellite. J. Geophys. Res. 98, 10713–10723, 1993.

Hays, P.B., Wu, D.L., the HRDI science team Observations of the diurnal tide from space. J. Atmos. Sci. 51, 3077–3093, 1994.

Killeen, T.L., Skinner, W. R., Johnson, R.M., et al. TIMED Doppler Interferometer (TIDI), in: Larar, Allen M. (Ed.), Optical Spectroscopic Techniques and Instrumentation for Atmospheric and Space Research III. Proceedings of SPIE 3756, pp. 289–301, 1999.

Lellouch, E., Goldstein, J.J., Bougher, S.W., et al. First absolute wind measurements in the middle atmosphere of Mars. Astrophys. J. 383, 401–406, 1991.

Limpasuvan, V., Wu, D.L., Schwartz, M.J., et al. The two-day wave in EOS MLS temperature and wind measurements in 2004–2005. Geophys. Rev. Lett. 32, L17809, doi:10.1029/2005GL02339, 2005.

Mason, A.H., Meek, C., Hagan, M.E., et al. Seasonal variations of the semi-diurnal and diurnal tides in the MLT: multi-year MF radar observations from 2–70°N, modelled tides (GSWM, CMAM). Ann. Geophys. 20, 661–677, 2002.

Nozawa, S., Iwahashi, H., Brekke, A., et al. The quasi 2-day wave observed in the polar mesosphere: comparison of the characteristics observed at Tromso and Poker Flat. J. Geophys. Res. 108 (D24), 4748, doi:10.1029/2002JD00322, 2003.

Palo, S.E., Roble, R.G., Hagan, M.E. Middle atmosphere effects of the quasi-two-day wave determined from a General Circulation Model. Earth Planet. Space 51, 629–647, 1999.

Riggin, D.M., Lieberman, R.S., Vincent, R.A., et al. The 2-day wave during the boreal summer of 1994. J. Geophys. Res. 109, D08110, doi:10.1029/2003JD00449, 2004.

Schwartz, M.J., Read, W.G., Snyder, W.V. Polarized radiative transfer for Zeeman-split oxygen lines in the EOS MLS forward model. IEEE Trans. Geosci. Remote Sensing 44 (5), 1182–1191, 2006.

Talaat, E.R., Lieberman, R.S. Nonmigrating diurnal tides in mesosphere and lower thermospheric winds and temperatures. J. Atmos. Sci. 56, 4073–4087, 1999.

Waters, J.W., Froidevaux, L., Harwood, R.S., et al. The Earth Observing System Microwave Limb Sounder (EOS MLS) on the Aura satellite. IEEE Trans. Geosci. Remote Sensing 44 (5), 1075–1092, 2006.

Wu, D.L., Hays, P.B., Kinner, W.R.S. A least squares fitting method for spectral analysis of space–time series. J. Atmos. Sci. 52, 3501–3511, 1995.